Available online at www.sciencedirect.com

ScienceDirect

Physics Procedia 67 (2015) 270 – 275

Physics Procedia

25th International Cryogenic Engineering Conference and the International Cryogenic Materials Conference in 2014, ICEC 25–ICMC 2014

Thermal property measurements of critical materials for SPICA payload module

Keisuke Shinozaki[a,*], Tadahito Mizutani[a], Takenori Fujii[b], Takashi Onaka[c], Takao Nakagawa[d], Hiroyuki Sugita[a]

[a]*Aerospace Research and Development Directorate, JAXA, 2-1-1, Sengen, Tsukuba city, Ibaraki, 305-0085, Japan*
[b]*Cryogenic Research Center, University of Tokyo, 2-11-16, Yayoi, Bunkyo-ku, Tokyo, 113-0032, Japan*
[c]*Department of Astronomy, University of Tokyo, 7-3-1, Hongo, Bunkyo-ku, Tokyo, 113-0033, Japan*
[d]*Institute of Space and Astronautical Science, JAXA, 3-1-1, Yoshinodai, Chuo-ku, Sagamihara city, Kanagawa, 252-5210, Japan*

Abstract

The Space Infrared Telescope for Cosmology and Astrophysics (SPICA) is a pre-project of JAXA in collaboration with ESA to be launched around 2025. The 3m-class infrared telescope must be below 6K, based on scientific requirements, and features effective radiant cooling into deep space at L2 point combined with a mechanical cooler system in order to cool scientific instruments as well as the telescope. The thermal design of the SPICA payload module must involve researching and measuring the thermophysical properties of materials in order to achieve a highly reliable cooling chain. Accordingly, all critical materials, particularly FRPs were determined and their thermal properties (thermal conductivity, specific heat, and thermal expansion) measured. Subsequently, the measured values were compared with those in literature and included in a thermal model analysis. This paper introduces details of these thermal properties measurements, comparisons with values in literature, and a thermal model analysis of the SPICA payload module.

Peer-review under responsibility of the organizing committee of ICEC 25-ICMC 2014

Keywords: SPICA; thermal conductivity;, specific heat;, TE;, FRP;, Al alloy;

1. Introduction

Most space cryogenic missions wish to optimize thermal and structural designs to reduce the heat load on mission instruments as well as the mass of the mission payload with an appropriate design with respect to the mechanical load during launch. However, the general lack of low-temperature physical property is always a major concern in space cryogenics design, and measuring the physical property of a critical material sample is essential, except when a design margin is included to some extent (Shaughnessy et al. (2007); McDonald et al. (2006)).

* Corresponding author. Tel.: +81-50-3362-4607 ; fax: +81-29-868-5969.
E-mail address: shinozaki.keisuke@jaxa.jp

Peer-review under responsibility of the organizing committee of ICEC 25-ICMC 2014
doi:10.1016/j.phpro.2015.06.086

This paper describes the mission activity to obtain the low-temperature thermophysical properties of material used in the payload module in order to mitigate the high risk and reliably meet the thermal requirements in the SPICA mission.

2. Conceptional design of the payload module

The SPICA payload module (PLM) adopts a new-concept cryogenic system that uses no stored cryogen to meet advanced mission requirements (Shinozaki et al. (2014)). One of the important thermal requirements for the PLM is that the SIA (Scientific Instrument Assembly) must be cooled to below 6 K. SIA includes the telescope assembly as well as scientific instruments. This requirement is based on the scientific SPICA requirement, which provides superior sensitivity with a low thermal background. SIA has a combined cooling system featuring mechanical and efficient radiative forms of cooling in a stable thermal environment at the Sun-Earth L2. The SIA is surrounded by a baffle, a telescope shell, three shields (inner, middle and outer) and a sun shield to reduce the radiative heat flow from the outer environment. The radiator portions on the +X and -X sides of each shield dissipate most absorbed heat from the sun and the spacecraft bus module (BM) into deep space. Thermal shields should have proper thermal conductance to transfer heat to the radiator, and must need to achieve proper structural requirements.

The SIA, the telescope shell and three shields are structurally supported by the BM with the main truss between them. Because the main truss was the main contributor of heat load at the 4.5 K stage, the separation mechanism with the spring support is located at the telescope shell interface (Mizutani et al. (2014)). The spring is mechanically fixed during launch, and helps support the SIA mechanically and reduce the parasitic heat load with a small cross-section after operating the separation mechanism. The heat load through the main truss assembly with the separation mechanism has been limited to within 5 mW, which corresponds to 1/4 of the heat load without the separation mechanism.

3. Materials used in the payload module

Table 1. Materials used in the payload module. Low-k CFRP : prepreg T700 and T300 (Toray), Low-k CFRP 2nd : prepreg T700, Low-k CFRP 3rd : prepreg T700 (different lamination), High-k CFRP : prepreg E9025C-25N (Nippon Graphite Fiber Corporation), Al-FRP : Al fiber HT-10-3K (Taimei Chemicals Co.Ltd.). The low-k CFRP-2nd samples were fabricated in order to measure and compare to the low-k CFRP samples.

1) TC : Thermal conductivity measurement (3∼300 K).
2) SH : Specific heat measurement (3∼300 K).
3) CTE : Coefficient of thermal expansion measurement (120∼300 K).
◎ : measured and updated in the thermal model analysis, ○ : measured.

Material	Application	Temperature region	TC[1)]	SH[2)]	CTE[3)]	Note
Al-alloy A1050	Thermal shield	10 ~ 150 K	○			
Al-alloy A6061	Thermal shield	10 ~ 150 K	○			
Al-alloy A6063	Thermal shield	10 ~ 150 K	○			
Al-alloy ST-60	Thermal shield	10 ~ 150 K	○			Option
Low-k CFRP	Main truss	4 ~ 30 K	○	○	◎	
Low-k CFRP-2nd			○	○	○	for reference
Low-k CFRP-3rd	Truss separation spring	4 ~ 30 K	○			
High-k CFRP	Thermal shield	10 ~ 150 K	○	○	◎	Option
Al-FRP	Main truss	30 ~ 250 K	◎	○	◎	
GFRP	Thrust truss	15 ~ 210 K	○			
Manganin	Harness	4 ~ 300 K				
Ph-Br	Harness	4 ~ 300 K				
SUS304	Harness	4 ~ 300 K				
Teflon	Harness	4 ~ 300 K				

As described in Sec. 2, the physical properties of materials used in the thermal structure design must be accurately obtained in order to ensure reliable conformance with the SIA temperature requirement for the SPICA payload

module. In particular, the thermal properties (thermal conductivity, specific heat and coefficient of thermal expansion) significantly impact on the feasibility of the low temperature design including the initial cooling from room temperature to below 6K after launch, the SIA alignment design, and the heat load on the SIA.

Table 1 lists materials proposed for use in the payload module thermal structure design. Al-alloy and FRP material are mainly used for the thermal shield and the main truss. CFRP is used for the lower truss between 6 and 30 K (SIA and the telescope shell), and Al-FRP (Alumina fiber composite) is used for the middle truss between 30 and 100 K (the telescope shell and the outer shield I/F), and the upper truss between 100 and 250 K (the outer shield I/F and the Bus module I/F). These selections are based on the typical behavior of various types of FRPs (Hirabayashi et al. (2008)). Most harness materials for a heater, thermometer and instrument mainly comprise manganin, while 304 stainless steel (SUS304) is used as an EMC shield material. A Ph-Br material is used for the current lead between 6 and 300 K for the superconducting magnet of the adiabatic demagnetization refrigerator (Duband et al. (2014)), while Teflon is considered for the shield material of these harnesses.

In the SPICA study, the thermal properties of these materials were researched, measured and included in the thermal model via the following processes.

- The thermophysical values for all materials were researched from a range of literature.
- The reference values of higher thermal conductivity in this literature were used for the material, except the high-k CFRP and Al-alloys in the thermal design.
- The reference values of lower thermal conductivity in this literature were used for Al-alloys in the thermal design.
- Unreliable thermal property materials were determined.
  - Few literatures, or significant discrepancies between each piece of literature.
  - Reference papers used are old (pre-1960s, for example).
- Samples of determined materials are fabricated and measured.
- Compared and newly included in the thermal model.

The thermal properties of FRP materials strongly depend on the fiber, plastic, volume fraction (Vf), orientation direction of each layer, manufacturing processes and so on. Fig. 1 compares thermal conductivity in GFRP literature based on the research, showing significant differences between them. The value of Takeno et al. (1986), as shown by a blue inverted triangle (|| direction) is used to indicate GFRP thermal conductivity in the current payload module thermal design, because it shows higher thermal conductivity in comparison with other values except Ross Jr (2004)(red solid box), made of S-glass. Accordingly, the measured value of the GFRP sample fabricated in this study showed drastically lower thermal conductivity (Mizutani et al. (2014)).

Following reference research, critical materials determined to measure these thermal properties were determined. Table 1 lists each measurement. All FRP material was measured due to the uncertainty discussed above, while the thermal conductivity of Al-alloys was also measured to compare reference values.

4. Thermal property measurement

The thermal conductivities of these material samples were measured using the Physical Property Measurement System (PPMS, Quantum Design, Inc.) in collaboration with the cryogenic research center at the University of Tokyo. The samples were $8 \times 2 \times 2$ mm in size. The temperature range was basically $3 \sim 300$ K and the electrical resistivity was also measured simultaneously. The specific heat of these samples was also measured using the PPMS, and the sample was $4 \times 4 \times 1 \sim 5$ mm in size. The measurement error was typically $5 \sim 10$ %, which was dominated by systematic error in the temperature reduction, temperature calibration accuracy, and the heat capacity of the sample base plate.

The coefficient of thermal expansion (CTE) was measured using the laser interferometer in the Toray research center. The sample was $5 \times 5 \times 10$ mm in size. The temperature range of all the sample was $120 \sim 300$ K with constant temperature increase / decrease of 2 K / min. The typical measurement accuracy was 0.1×10^{-6}/K.

In this study, another CFRP samples (CFRP-2nd) were also measured as a reference for comparison to the CFRP candidate result for the main truss. In addition, the CFRP candidate for the truss separation spring (CFRP-3rd) showed

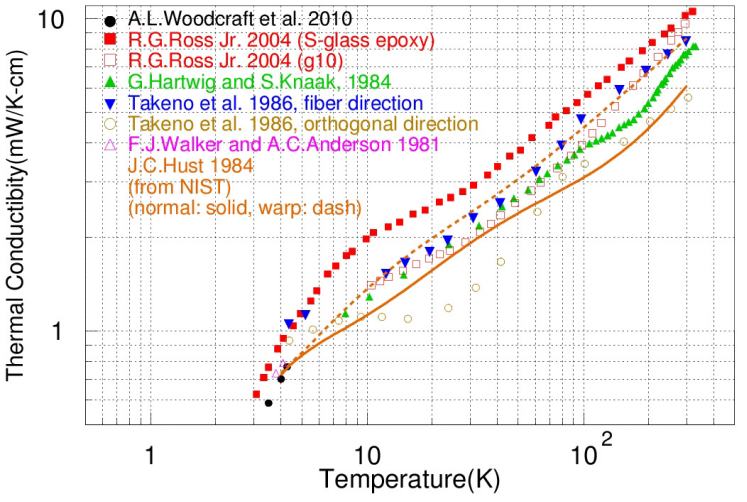

Fig. 1. Comparison of thermal conductivity of GFRP references (log-log). Black solid circle : Woodcraft et al. (2010)(Permaglass ME771), Red solid box : Ross Jr (2004)(S-glass epoxy), Red open box : Ross Jr (2004)(G10), Green solid triangle : Hartwig and Knaak (1984)(E-qglass epoxy), Blue solid inverted triangle : Takeno et al. (1986)(E-glass, araldite)(|| direction), Yellow open circle : Takeno et al. (1986)($\perp$ direction), Purple open triangle : Walker and Anderson (1981)(G10CR). Orange line : Hust (1984) Child et al. (1973)(fromNIST, G10CR epoxy) (solid : || direction, dash : $\perp$ direction).

a different material from the CFRP for the main truss, due to the thermal structure study of the spring design (Mizutani et al. (2014)).

5. Revision of the payload module thermal design

Most results were favorable and had little impact on the payload module thermal design, like to the FRP specific heat shown in Fig. 3 (Shinozaki et al. (2014)). Then, one of the most critical result was the thermal conductivity of the High-k CFRP. Three CFRP samples were measured and all of which showed higher thermal conductivity than low-k CFRP between 5 and 300 K as shown in Fig. 2. However, the targets were 78 and 850 mW/K/cm at 4 and 90 K respectively in past thermal designs; based on the thermal conductivity of the proposed carbon fiber itself. Therefore, the measured value was over 10 times lower than the target value and we decided to replace the thermal shield design from the combination of panel and frame using the high-k CFRP to the Al-alloy honeycombed structure, while another material sample of the high-k CFRP material was under measurement.

Five Al-FRP samples in total were measured and the variance between them was around 10 %. Sample 4 has the highest measured value, plotted in Fig. 2, with thermal conductivity exceeding the reference values between 20 and 100 K. Hence, the Al-FRP thermal conductivity in the thermal design was replaced from the value of Takeno et al. (1986)(|| direction) to the measured value, and the heat load on the SIA becomes 0.5 mW larger.

One of the critical issues for the thermal study was the specific heat of the FRP material, which influenced the required initial cooling time after launch. Fig. 3 shows the measured specific heat of FRP materials. All measured values of all FRP samples were lower than the G-10 reference value used in past thermal model analysis before these measurements. Accordingly, we concluded that it was better to use the G-10 reference value in order to provide a design margin for the thermal transient analysis during the initial cooling.

Finally, the measured CTE of FRP samples was included in the thermal strain analysis of the payload module. There was concern at the thermal strain under low temperature for the interface between the upper truss and the tele-

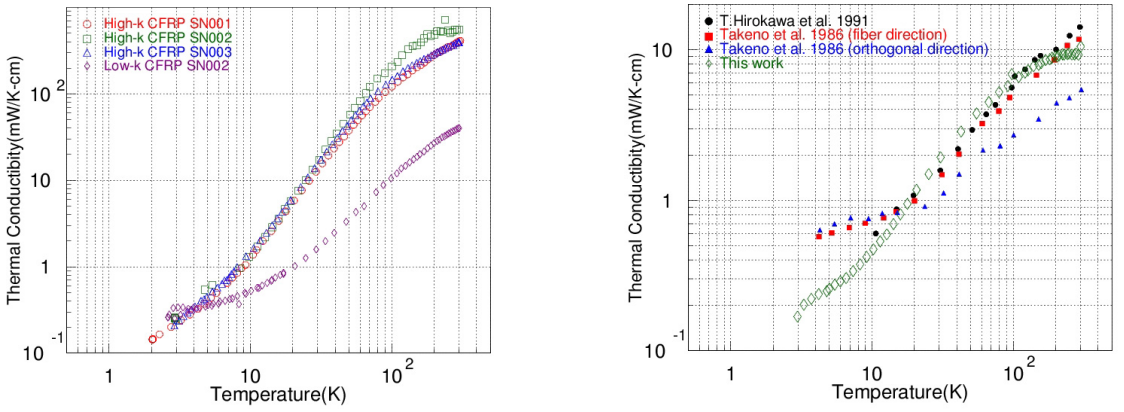

Fig. 2. Left : Comparison between the measured thermal conductivity of high-k CFRPs and the low-k CFRP (log-log). Black open circle : High-k CFRP sample 1, Red open box : High-k CFRP sample 2, Blue open triangle : High-k CFRP sample 3, Purple open diamond : Low-k CFRP Smaple 2. Right : Comparison between the measured thermal conductivity of Al-FRP materials and references (log-log). Black solid circle : Hirokawa et al. (1991)(T300, epoxy), Red solid box : Takeno et al. (1986)(Sumitomo Chemical Alumina, Araldite)(|| direction), Blue solid triangle : Takeno et al. (1986)(⊥ direction), Green open diamond : This work.

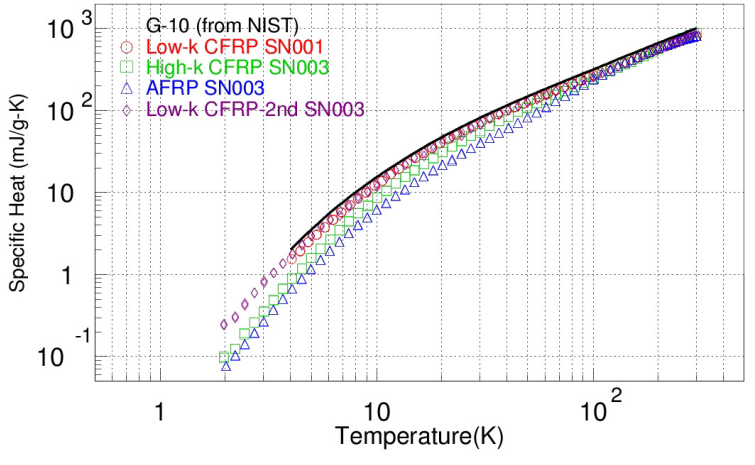

Fig. 3. Comparison between the measured specific heat of FRP materials and G-10 references (log-log). Black line : G-10 (NIST), Red open circle : Low-k CFRP sample 1, Green open box : High-k CFRP sample 3, Blue open triangle : Al-FRP sample 3, Purple open diamond : Low-k CFRP-2nd sample 1.

scope shell. However, the measured CTE of FRP samples was lower than the CTE of Al-alloy, and it was analytically confirmed that the effect of CTE of FRP on the thermal strain at the interface was negligible, even when the individual variability of the measured samples was considered.

6. Conclusion

The following results were obtained in this activity.

- Thermophysical values for all proposed material in the SPICA payload module were researched from a range of literatures, and critical materials which should be measured were determined.
- The thermophysical properties of all FRP materials and Al-alloy were measured and compared to other reference values.
- The measured value of the high-k CFRP sample was over 10 times lower than the target value, and the thermal shield design was replaced with an Al-alloy honeycombed structure instead of using the high-k CFRP material.
- The thermal conductivity of Al-FRP material in the thermal design was updated to the measured value.
- All measured specific heat of FRP samples was lower than the G-10 reference value used in past thermal model analysis, and we confirmed that it was better to use the G-10 reference value in order to provide a design margin for the payload module.

For the SPICA mission, the thermal properties of thermal structure materials have been sufficiently understood by research and these measurements, which provides for high reliability and feasibility for the SPICA payload module design. Accordingly, following this risk mitigation activity, a phase-up review of the mission is expected.

Acknowledgements

The authors deeply appreciate all members of the SPICA pre-project team and the cryogenic group in Sumitomo Heavy Industry. Ltd., Niihama works for their support for this work.

References

Child, G., Erics, L., Powell, R., 1973. Thermal Conductivity of Solids at Room Temperature and Below. NBS Monograph 131.

Duband, L., Duval, J., Luchier, N., 2014. SAFARI Engineering Model 50 mK Cooler. Cryogenics Accepted.

Hartwig, G., Knaak, S., 1984. Fibre-epoxy composites at low temperatures . Cryogenics 24, 639–647. E-glass, epoxy.

Hirabayashi, M., Narasaki, K., Tsunematsu, S., Kimura, Y., Yoshida, S., Murakami, H., Nakagawa, T., Ohnishi, A., Matsumoto, T., Kaneda, H., 2008. Thermal design and its on-orbit performance of the AKARI cryostat. Cryogenics 48, 189–197.

Hirokawa, T., Yasuda, J., Iwasaki, Y., Noma, K. Nishijima, S., Okada, T., 1991. Design of support strap with advanced composite for cryogenic application. Cryogenics 31, 288–291. T300, epoxy, Vf50%.

Hust, J., 1984. Thermal Conductivity of Glass Fiber/Epoxy Composite Support Bands For Cryogenic Dewars. Phase II NBS, Boulder.

McDonald, P.C., Jaramillo, E., Baudouy, B., 2006. Thermal design of the CFRP support struts for the spatial framework of the Herschel Space Observatory. Cryogenics 46, 298–304. T300, epoxy, Vf60%, for Herschel.

Mizutani, T., Yamawaki, T., Komatsu, K., Goto, K., Takeuchi, S., Shinozaki, K., 2014. Preliminary structural design and key technology demonstration of cryogenic assembly in the next-generation infrared space telescope SPICA, in: Proc. SPIE, 9143, Space Telescopes and Instrumentation 2014 Optical, infrared, and Millimeter Wave.

NIST, . Cryogenics home page. Http://cryogenics.nist.gov/MPropsMAY/materialproperties.htm.

Ross Jr, R.G., 2004. Estimation of thermal conduction loads for structural supports of cryogenic spacecraft assemblies. Cryogenics 44, 421–424. T300.

Shaughnessy, B.M., Eccleston.P., Fereday, K., Canfer, S., Norgaard-Nielsen, H., Jessen, N., 2007. Thermal conductivity measurement below 40K of the CFRP tubes for the Mid-Infrared Instrument mounting struts. Cryogenics 47, 348–352. T300-K6, bakelite, Vf56%, for JWST.

Shinozaki, K., Sato, Y., Sawada, K., Ando, M., Sugita, H., Yamawaki, T., Mizutani, T., Komatsu, K., Nakagawa, T., Murakami, H., Matsuhara, H., Takada, M., Takai, S., Okabayashi, A., Tsunematsu, S., Kanao, K., Narasaki, K., 2014. Thermal study of payload module for the next-generation infrared space telescope SPICA in risk mitigation phase. Cryogenics Accepted.

Takeno, M., Nishijima, S., Okada, T., Fujioka, K., Kuraoka, Y., 1986. Thermal and Mechanical Properties of Advanced Composite Materials at Low temperatures. Cryogenic Engineering 12, 182–187. CFRP(T300), AFRP(T300), GFRP(E-glass), Araldite, Vf50%).

Walker, F.J., Anderson, A.C., 1981. Thermal conductivity and specific heat of a glass-epoxy composite at temperature below 4K. Review of Scientific Instruments 52, 471–472. NIMA G-10CR, parallel to the glass fabric.

Woodcraft, A., Martelli, V., Ventura, G., 2010. Thermal conductivity of ME771 glass-epoxy laminate from millikelvin temperature to 4K. Cryogenics 50, 52–54. Permaglas ME771.